






Tree differences in primary and secondary growth drive convergent scaling in leaf area to sapwood area across Europe

Giai Petit¹ , Georg von Arx^{2,3}, Natasa Kiorapostolou^{1,4}, Silvia Lechthaler¹ , Angela Luisa Prendin¹ , Tommaso Anfodillo¹, Maria C. Caldeira⁵, Hervé Cochard⁶, Paul Copini^{4,7} , Alan Crivellaro¹, Sylvain Delzon⁸ , Roman Gebauer⁹, Jožica Gričar¹⁰, Leila Grönholm¹¹, Teemu Hölttä¹¹, Tuula Jyske¹², Martina Lavrič¹⁰, Anna Lintunen¹¹, Raquel Lobo-do-Vale⁵, Mikko Peltoniemi¹², Richard L. Peters², Elisabeth M. R. Robert¹³, Sílvia Roig Juan¹², Martin Senfeldr⁹, Kathy Steppe¹⁴, Josef Urban^{9,15}, Janne Van Camp¹⁴ and Frank Sterck⁴

¹Departamento TeSAF, Università degli Studi di Padova, Viale dell'Università 16, 35020 Legnaro (PD), Italy; ²Swiss Federal Institute for Forest, Snow and Landscape Research (WSL), Zürcherstrasse 111, 8903 Birmensdorf, Switzerland; ³Institute for Environmental Sciences, University of Geneva, 24 rue du Général-Dufour, 1211 Geneva, Switzerland; ⁴Department of Environmental Sciences, Wageningen University, Droevendaalsesteeg 3, NL 6700 AA Wageningen, the Netherlands; ⁵Forest Research Centre (CEF), School of Agriculture, University of Lisbon, Tapada da Ajuda, 1349-017 Lisbon, Portugal; ⁶Université Clermont-Auvergne, INRA, PIAF, Site de Crouël 5, chemin de Beaulieu, 63000 Clermont-Ferrand, France; ⁷Wageningen Environmental Research (Alterra), Wageningen University & Research Wageningen, Droevendaalsesteeg 3, NL 6700 AA Wageningen, the Netherlands; ⁸INRA, University of Bordeaux, UMR BIOGECO, Avenue des Facultés, Talence FR 33405, France; ⁹Dept. of Forest, Botany, Dendrology and Geobiocenology, Mendel University in Brno, Zemedelska 3, 61300 Brno, Czech Republic; ¹⁰Slovenian Forestry Institute, Vecna pot 2, SI – 1000 Ljubljana, Slovenia; ¹¹Department of Forest Sciences, University of Helsinki, Latokartanonkaari 7, FI 00014 Helsinki, Finland; ¹²Natural Resources Institute Finland (Luke), Latokartanonkaari 9, FI-00790 Vantaa, Finland; ¹³CREAF, Cerdanyola del Vallès 08193, Spain; ¹⁴Laboratory of Plant Ecology, Faculty of Bioscience Engineering, Ghent University, Coupure links 653, BE-9000 Ghent, Belgium; ¹⁵Siberian Federal University, Svobodnyy Ave 79, 660041 Krasnoyarsk, Russia

Summary

Author for correspondence:

Giai Petit

Tel: +39 827 2689

Email: giai.petit@unipd.it

Received: 25 October 2017

Accepted: 16 February 2018

New Phytologist (2018) **218**: 1383–1392

doi: 10.1111/nph.15118

Key words: allocation, climate change, functional balance, leaf area, plant architecture, sapwood, structural balance, xylem.

- Trees scale leaf (A_L) and xylem (A_X) areas to couple leaf transpiration and carbon gain with xylem water transport. Some species are known to acclimate in $A_L : A_X$ balance in response to climate conditions, but whether trees of different species acclimate in $A_L : A_X$ in similar ways over their entire (continental) distributions is unknown.
- We analyzed the species and climate effects on the scaling of A_L vs A_X in branches of conifers (*Pinus sylvestris*, *Picea abies*) and broadleaved (*Betula pendula*, *Populus tremula*) sampled across a continental wide transect in Europe.
- Along the branch axis, A_L and A_X change in equal proportion (isometric scaling: $b \sim 1$) as for trees. Branches of similar length converged in the scaling of A_L vs A_X with an exponent of $b = 0.58$ across European climates irrespective of species. Branches of slow-growing trees from Northern and Southern regions preferentially allocated into new leaf rather than xylem area, with older xylem rings contributing to maintaining total xylem conductivity.
- In conclusion, trees in contrasting climates adjust their functional balance between water transport and leaf transpiration by maintaining biomass allocation to leaves, and adjusting their growth rate and xylem production to maintain xylem conductance.

Introduction

In vascular plants, leaf hydraulics play a key role for the whole plant physiology. Leaf hydration is fundamental to keep stomata open and maintain gas exchange and carbon fixation through photosynthesis. Bulk water moves passively against gravity from fine roots in the soil to the pores of mesophyll cells in the leaves following a water pressure gradient, and a vapor pressure gradient between stomatal cavities and atmosphere. Therefore, the rate of water flowing from roots to leaves (F , $\text{cm}^3 \text{s}^{-1}$) and transpired by the leaves (ET , $\text{cm}^3 \text{s}^{-1}$) depends primarily on the vapor pressure deficit of the atmosphere (VPD, MPa) and on the soil water potential (Ψ_{soil} , MPa) (Zweifel *et al.*, 2005). In parallel, F and

ET are constrained by the frictional forces opposed by the different conductive structures along the pathway from roots to leaves (Tyree & Zimmermann, 2002). Of these structures, the xylem of roots, stem and branches accounts for the hydraulic path length, and thus represents an increasing construction cost for the carbon balance of taller trees (Mencuccini *et al.*, 2007). A key hydraulic property of the whole plant is the leaf-specific conductance, that is, the condition that allows water flowing through the xylem to replenish water lost through leaf transpiration (functional balance).

According to metabolic scaling theory, trees are predicted to converge towards universal allometric scaling amongst plant structures, described by (Banavar *et al.*, 1999; West *et al.*, 1999):

$$Y = a \cdot X^b \quad \text{Eqn 1}$$

(X and Y , two structural/functional traits (e.g. leaf and xylem biomass); a , allometric constant; b , scaling exponent.)

The functional balance of $ET = F$ is typically reflected in the widely observed isometric relationship (i.e. scaling exponent $b \sim 1$) between leaf area (A_L) and sapwood area (A_S) (Grier & Waring, 1974; Kaufmann & Troendle, 1981; Shelburne *et al.*, 1993), suggesting that A_L and A_S increase in equal proportion with increasing plant size. However, different conditions in atmosphere (VPD) and soil (Ψ_{soil}) may affect the transpiration from the leaves and the water flow in the xylem. Indeed, environmental variability can induce modifications at different scales, from biochemistry to structural properties, that allow trees to maintain the functional water balance ($ET = F$) and to attain a positive carbon balance (i.e. carbon gain through photosynthesis minus carbon expenses for maintenance and growth). These responses may require changes in the carbon allocation to leaves vs sapwood (Mencuccini, 2014; Mitchell *et al.*, 2014; Petit *et al.*, 2016; Sterck & Zweifel, 2016). For instance, if less soil water is available (lower Ψ_{soil}) or air humidity increases (lower VPD) (Tullus *et al.*, 2012), K is expected to increase to maintain a given leaf transpiration rate. On the contrary, higher xylem tensions developing with increasing VPD would result in higher risk of embolism formation, unless a stronger stomatal control on ET is opposed, with consequent positive effects on xylem safety, but negative impacts on carbon assimilation and on the overall carbon balance (McDowell *et al.*, 2008). Water conduction under tension (negative pressure drop) exposes xylem conduits to the risk of embolism formation and reduction in the overall xylem conductance. A certain degree of xylem embolization occurs continuously in several species (Nardini *et al.*, 2011), but can become irreversible under extreme drought conditions or after freeze–thaw cycles (Tyree & Zimmermann, 2002; Cochard, 2006). The resistance to embolism formation is a key feature for hydraulic safety and can be conferred by different anatomical properties at the cell level, but it is unlikely that high xylem conductivity is associated with high embolism resistance (Hacke & Sperry, 2001; Gleason *et al.*, 2016). This means that maintaining the functional balance ($ET = F$) while prioritizing safety or efficiency, likely implies that the carbon costs of producing an equally conductive xylem would change accordingly. Because many plant species have distribution ranges covering different climatic regions, it can be expected that evolution selected for different structural balances in leaf area vs sapwood area across regions, and also during the different phases of ontogeny.

It has been commonly observed that both trees under environmental (Mencuccini & Grace, 1995; Martínez-Vilalta *et al.*, 2009; Sellin *et al.*, 2017) or size-related stress conditions (McDowell *et al.*, 2002) decrease the ratio of leaf area to sapwood area ($A_L : A_S$), likely to increase the leaf specific conductance. However, the patterns of anatomical and hydraulic properties related to tree size very seldom are considered in these types of studies. In particular, sapwood is not an homogeneous tissue within a tree (Spicer & Gartner, 2001). Sapwood conductivity

increases from the stem apex towards the base as a consequence of the basal widening of xylem conduits (Anfodillo *et al.*, 2013), and increases from pith to bark as a consequence of the increase in conduit size in younger rings due to the effect of longitudinal growth (Carrer *et al.*, 2015). The general architectural design of the xylem implies that narrower and generally safer conduits (Hacke *et al.*, 2006, 2017) occur close to the transpiring leaves, where tension is highest. Below, conduits progressively increase in diameter (Anfodillo *et al.*, 2013), thus confining most of the total hydraulic resistance within a short distance from the apices of stem and branches (Petit & Anfodillo, 2009; Petit *et al.*, 2010). In addition, longer xylem path lengths in taller trees and limitations to photosynthesis imply that maintenance costs and biomass production are more expensive on a leaf area basis (Buckley & Roberts, 2006; Anfodillo *et al.*, 2016). In this respect, it has been shown that larger leaf biomass can be sustained along branches under drier conditions when the annual investment in primary and secondary growth is reduced, and more rings contribute to the total sapwood conductance (Petit *et al.*, 2016; Sterck & Zweifel, 2016).

In the present study, we tested the hypothesis that selection favored tree species converging towards similar scaling of leaf area vs functional xylem area. We investigated the structural variation of leaf area to xylem area accounting for the effect of the axial length in four species – two conifers and two broadleaved – across a wide latitudinal gradient across Europe that almost completely covers their latitudinal distribution. We hypothesized that trees are selected to have similar structural balances (i.e. similar combinations of leaf and sapwood areas) in branches, thus expecting convergence towards a similar exponent (b) for the scaling relationship between A_L and A_S , at least at the species level. We expected regional effects on such scaling trends, because variation in rainfall, temperature and drought may affect structural balances in trees. Moreover, we analyzed the variation of A_L and A_S along the branch and expected their axial scaling to be isometric ($b = 1$) and similar to the scaling of total leaf area vs sapwood area at the stem base in trees of different sizes. Lastly, we tested the hypothesis (Petit *et al.*, 2016) that trees with slow branch elongation rates allow a relatively higher investment in leaf mass than sapwood mass by accumulating sapwood rings over more successive years than fast growing trees, which could compensate for the lower allocation to xylem.

Materials and Methods

Geographical range and sampling material

We selected sites along a wide geographical transect of $> 27^\circ$ of latitude from Southern to Northern Europe, thus covering a wide range of environments: mountain Mediterranean forest (Portugal, POR, $40^\circ\text{N } 7^\circ\text{E}$); mountain mixed forest (Switzerland, CH, $46^\circ\text{N } 7^\circ\text{E}$, and Italy, IT, $46^\circ\text{N } 12^\circ\text{E}$); central mixed forest (Czech Republic, CZ, $49^\circ\text{N } 16^\circ\text{E}$); Atlantic mixed forest (the Netherlands, NL, $52^\circ\text{N } 6^\circ\text{E}$); low and high latitude boreal forests (Southern Finland, FI_S, $60^\circ\text{N } 25^\circ\text{E}$, and Northern Finland,

FI_N, 67°N 29°E, respectively) (Fig. 1). These sites are characterized by different climatic conditions (Table 1).

We identified four target species whose distribution range is mostly or entirely covered by our latitudinal transect: two deciduous angiosperms (*Betula pendula* Roth. and *Populus tremula* L.) and two evergreen conifers (*Picea abies* Karst. and *Pinus sylvestris* L.). Sampling was conducted in each region before the end of the 2014 growing season to guarantee that we included most of the leaves and all of the xylem produced during that year by secondary growth. For each species and site, sun-exposed branches (to avoid shading effects) were cut between 2.6 and 8.9 m from the ground from four to 10 trees ranging from 5 to 30.2 m in height (Table 1). Some species were absent locally and therefore not sampled in all sites (Fig. 1; Table 1). For each branch, a segment was extracted at the fixed distance of $L = 70$ cm from the branch tip in order to standardize for the potential effects of the axial distance from the apex on xylem anatomy and on vessel or tracheid size in particular (Anfodillo *et al.*, 2013). All leaves/needles between the extracted segment and apex were collected and their dry biomass (M_L , g) was measured after drying them for 24 h in an oven at 60°C. On a representative subsample of 10–15 dry leaves and 30–40 needles, the weight (m_L , g) was

obtained, and their scanned images were analyzed with ImageJ (National Institutes of Health, Bethesda, MD, USA) for broadleaved and with ROXAS (von Arx & Carrer, 2014; Prendin *et al.*, 2017) for conifers for the assessment of leaf/needle area (a_L , m^2). Total branch leaf/needle area (m^2) was then assessed as $A_L = (a_L/m_L) \cdot M_L$. Hence, we refer to these branch samples as 70-cm branches in the remainder of the text.

For two sites, NL and FI_S, we tested for the effect of distance from the apex on the relationship between leaf area A_L and xylem area (A_X , mm^2) (Table 1). We therefore selected a subset of four branches per species for those two sites and sampled stem segments at distances (L) of 2, 10, 20, 60, 70 and 200 cm from the branch apex, and measured the leaf area between the apex and these sampling points. We did not observe any visual indication of heartwood in our branches, so we considered the whole xylem area to be conductive (i.e. the sapwood: $A_X = A_S$).

Wood anatomical measurements

Wood samples were embedded in paraffin (Anderson & Bancroft, 2002), and cut with a rotary microtome (Leica RM2245; Leica Biosystems, Nussloch, Germany) at 10–15 μm .

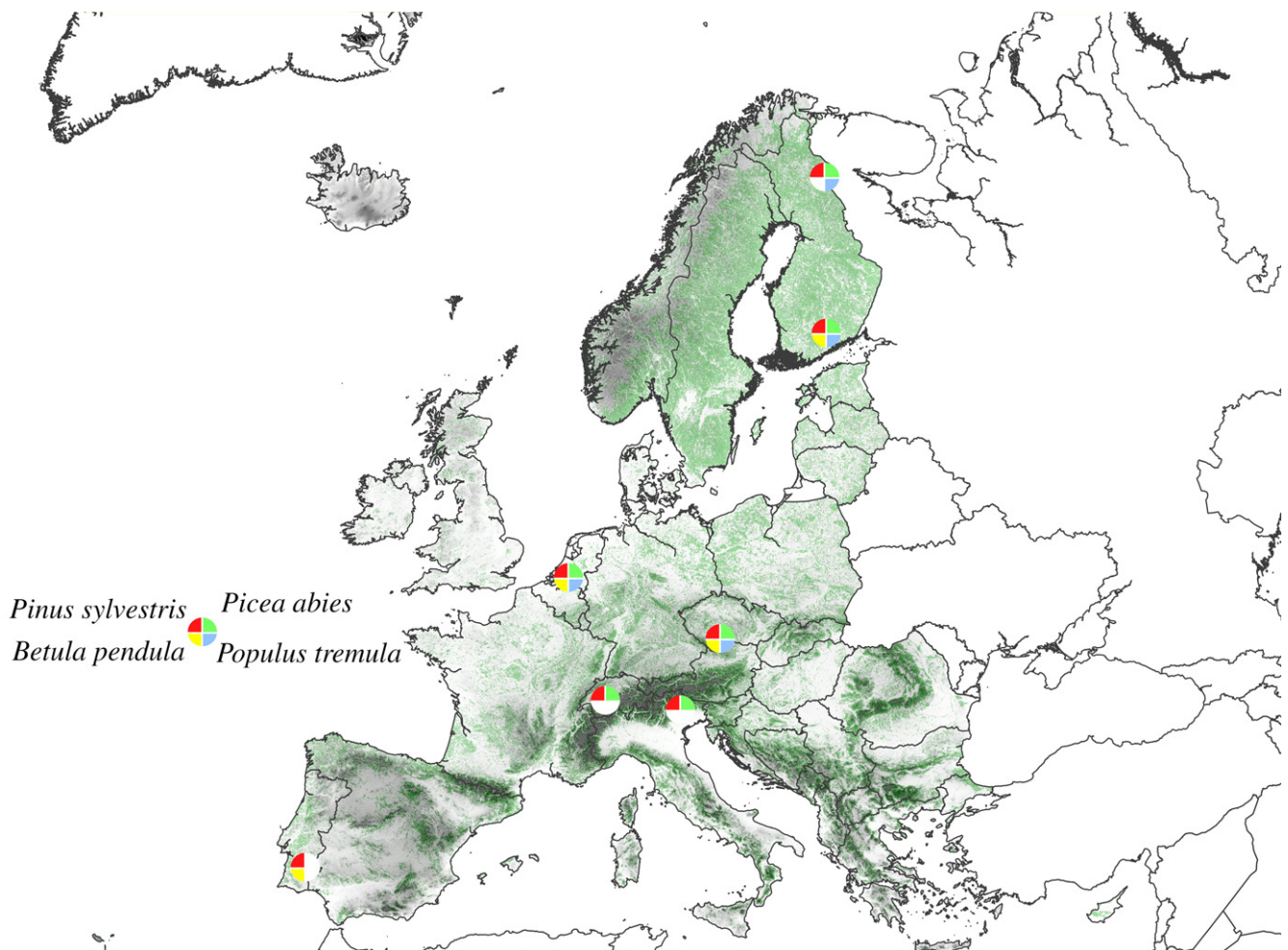


Fig. 1 Geographical distribution of sampling sites across Europe. Sampled species in the different regions are indicated with different colors. Green indicates forested areas.

Table 1 Descriptive information about sites (coordinates; MAT, mean annual temperature; MAP, mean annual precipitation; AI, aridity index = precipitation/potential evapotranspiration assessed for the period June–August) and sampled species (n , number of sampled trees; H , mean tree height; H_{cut} , height at which the sampled branch was cut along the stem; DBH, diameter at breast height)

| Region/species | Coordinates | Elevation (m asl) | MAT (°C) | MAP (mm) | AI | n^1 | $H \pm \text{SD}$ (m) | $H_{\text{branch}} \pm \text{SD}$ (m) | DBH \pm SD (cm) |
|-------------------------|-------------|-------------------|----------|----------|------|--------|-----------------------|---------------------------------------|-------------------|
| POR | 40°N 07°W | | | | | | | | |
| <i>Betula pendula</i> | | 1500 | 8 | 1725 | 0.27 | 8 | 9.3 \pm 2.1 | 3.9 \pm 0.7 | 12.1 \pm 2.5 |
| <i>Pinus sylvestris</i> | | 1450 | 8 | 1740 | 0.28 | 4 | 11.9 \pm 2.0 | 4.2 \pm 0.3 | 26.4 \pm 9.0 |
| CH | 46°N 12°E | | | | | | | | |
| <i>Picea abies</i> | | 1340 | 5 | 1315 | 0.35 | 9 | 23.7 \pm 5.3 | 5.5 \pm 1.4 | 64.1 \pm 26.1 |
| <i>P. sylvestris</i> | | 645 | 9 | 660 | 1.03 | 9 | 15.4 \pm 5.2 | 6.0 \pm 1.6 | 29.7 \pm 7.3 |
| IT | 46°N 16°E | 1075 | | | | | | | |
| <i>P. abies</i> | | | 7 | 1070 | 0.81 | 9 | 9.3 \pm 2.6 | 4.3 \pm 0.2 | 15.9 \pm 3.9 |
| <i>P. sylvestris</i> | | | 7 | 1070 | 0.81 | 10 | 7.0 \pm 1.8 | 4.3 \pm 0.4 | 17.4 \pm 4.3 |
| CZ | 49°N 16°E | 416 | | | | | | | |
| <i>B. pendula</i> | | | 8 | 575 | 0.47 | 10 | 6.9 \pm 1.3 | 4.6 \pm 0.5 | 7.3 \pm 2.5 |
| <i>Populus tremula</i> | | | 8 | 575 | 0.47 | 9 | 8.4 \pm 1.4 | 5.2 \pm 0.4 | 6.7 \pm 1.4 |
| <i>P. abies</i> | | | 8 | 575 | 0.47 | 10 | 7.7 \pm 1.0 | 4.9 \pm 0.3 | 11.0 \pm 1.8 |
| <i>P. sylvestris</i> | | | 8 | 575 | 0.47 | 10 | 6.9 \pm 1.5 | 4.5 \pm 0.5 | 8.7 \pm 2.1 |
| NL | 52°N 05°E | 5 | | | | | | | |
| <i>B. pendula</i> | | | 9 | 765 | 0.48 | 9 (3) | 15.6 \pm 4.7 | 6.0 \pm 1.8 | 24.0 \pm 15.4 |
| <i>P. tremula</i> | | | 9 | 765 | 0.48 | 8 (2) | 17.6 \pm 5.2 | 6.1 \pm 1.4 | 28.7 \pm 15.8 |
| <i>P. abies</i> | | | 9 | 765 | 0.48 | 10 (4) | 17.1 \pm 2.6 | 4.6 \pm 1.1 | 30.2 \pm 6.4 |
| <i>P. sylvestris</i> | | | 9 | 765 | 0.48 | 10 (4) | 10.7 \pm 3.2 | 5.8 \pm 1.0 | 19.0 \pm 14.7 |
| FI_S | 61°N 24°E | | | | | | | | |
| <i>B. pendula</i> | | 60 | 4 | 645 | 0.89 | 8 (2) | 8.2 \pm 3.3 | 5.1 \pm 0.8 | 6.4 \pm 2.8 |
| <i>P. tremula</i> | | 150 | 3 | 610 | 0.52 | 10 (4) | 7.8 \pm 1.6 | 4.4 \pm 1.0 | 6.9 \pm 1.4 |
| <i>P. abies</i> | | 140 | 3 | 610 | 0.52 | 9 (4) | 10.6 \pm 2.1 | 4.0 \pm 1.0 | 14.0 \pm 2.7 |
| <i>P. sylvestris</i> | | 140 | 3 | 610 | 0.52 | 9 (4) | 11.4 \pm 3.4 | 4.4 \pm 0.8 | 14.6 \pm 7.2 |
| FI_N | 67°N 29°E | | | | | | | | |
| <i>P. tremula</i> | | 370 | −2 | 545 | 0.07 | 9 | 7.8 \pm 1.7 | 4.0 \pm 0.5 | 8.0 \pm 1.8 |
| <i>P. abies</i> | | 405 | −2 | 545 | 0.07 | 9 | 7.9 \pm 1.7 | 4.1 \pm 0.6 | 12.5 \pm 4.2 |
| <i>P. sylvestris</i> | | 380 | −2 | 545 | 0.07 | 8 | 8.7 \pm 1.7 | 3.8 \pm 0.7 | 13.5 \pm 3.9 |

¹Number of branches used for extended sampling along the longitudinal axis is put between parentheses. asl, above sea level.

CH, Switzerland; CZ, Czech Republic; FI_N, _S, Finland North and South; IT, Italy; NL, the Netherlands; POR, Portugal.

Cross-sections were stained with safranin and AstraBlue (1% and 0.5% in distilled water, respectively) using standard methods (von Arx *et al.*, 2016), and slides permanently fixed with Eukitt (BiOptica, Milan, Italy). Slides were observed at $\times 40$ magnification under a light microscope with an integrated digital camera (Nikon Eclipse80i; Nikon, Tokyo, Japan). Overlapping images of the whole cross-section were stitched with PTGui (New House Internet Service BV, Rotterdam, the Netherlands). Analyses with ROXAS v.2.0 (von Arx & Carrer, 2014; Prendin *et al.*, 2017) were then performed on a wedge of known angle ($\alpha = 30\text{--}70^\circ$) centered at the pith, within which the area of each annual ring (A_R) was assessed. The total cross-sectional area of the xylem (A_X) was calculated as the sum of A_R of all of the rings multiplied by $360/\alpha$. Lastly, we calculated the mean branch elongation rate (ΔL) as the ratio of branch axial length (i.e. the cut distance of 70 cm from the apex) to its age (i.e. number of xylem rings at $L = 70$ cm).

Statistical analyses

Allometric scaling relationships were calculated by regressing the \log_{10} -transformed values for total $A_L(y)$ against \log_{10} -transformed values for $A_X(x)$, assumed to be fully functional ($A_X = A_S$, where

A_S is the sapwood area). The \log_{10} -transformation of independent (x) and dependent (y) variables resulted in normality and homoscedasticity. We first tested for a possible species effect on branch allometry, using a linear model with $\log_{10}(A_L)$ as the dependent variable, and $\log_{10}(A_X)$, species and the interaction (species and $\log_{10}(A_X)$) as independent variables. This model was run for all branches cut at 70 cm, and separately for the branches that were investigated for axial patterns (NL and FI_S). Afterwards, we added the regional effect and the interaction term with A_X both for the branches sampled at 70 cm from the apex and those from NL and FI_S sampled at different positions along the longitudinal axis. We compared the full model and all trimmed models, removing interaction terms and region or species effects after selecting the best (i.e. simplest) model based on AIC estimates using the maximum-likelihood method (Zuur *et al.*, 2009).

Finally, we compared our study branches with trees by adding all our branch samples to a subsample of trees from the BAAD dataset (Falster *et al.*, 2015), for which total leaf area and sapwood area (measured at stem base or at breast height) were given. We defined a categorical variable entity (tree or branch) to study the differences in allometric scaling between trees and branches. We tested whether branches differed from entire trees in

allometric scaling, using a linear model with $\log_{10}(A_L)$ as dependent variable, and $\log_{10}(A_X)$, entity (either branch or tree) and their interaction as independent factors. We compared the full model and the trimmed models, removing interaction term and entity effects, after performing an ANOVA to select the best (i.e. simplest) model. All analyses were run in R (R Development Core Team, 2014).

Results

Scaling of A_L vs A_X at 70 cm from the branch apex

For the branches sampled at 70 cm from the apex, species affected the y -intercept (i.e. the allometric constant a of Eqn 1), but not the slope (b) (Fig. 2a; Table 2). All species showed a similar slope of $b=0.58$, implying that A_X at $L=70$ cm from the apex varies proportionally more than the distal A_L . Instead, the actual leaf area for a given sapwood area in the branch significantly differed between species, as expressed by significant differences in the y -intercepts. The two conifer species had higher y -intercepts than the two broadleaved species, meaning that they pack a larger A_L for a given A_X . Remarkably, the branches of conifers also had a larger xylem area on average than the two broadleaved (Fig. 2a). Although adding region as an explanatory factor in the model significantly contributed to explaining the $\log_{10} A_L : \log_{10} A_X$ relationship, the explained variation (R^2) only increased from 0.73 to 0.75, which was attributed to differences between branches from NL and those from CZ and POR (Table 2; Fig. S1a). These minor regional impacts were not related to climate or other limiting growth (generally reflected in smaller ΔL) conditions, because the residuals from the predicted lines per species (Table 2; Fig. 2a) cannot be explained by the variation in TAP ($P=0.21$), MAP ($P=0.93$) AI ($P=0.77$) or ΔL ($P=0.71$) (Table S1; Fig. S1b).

For the same branches, branch elongation rate (ΔL) differed between sites (Fig. 3); the lowest ΔL occurred at the latitudinal extremes of our cross-European transect, that is, POR and FI_N. However, we did not find any significant relationship between ΔL and the meteorological variables (Table 2). We assessed the relationship between $\log_{10} \Delta L$ and $\log_{10} A_L : A_X$ for the different species, which was not significant for *P. tremula* and *P. sylvestris*, but resulted in a significant positive trend for *B. pendula* and a negative one for *P. abies* (Fig. 4a). In all species the annual allocation between leaves vs sapwood estimated from $(A_L/A_{X,OUT})$ (Fig. 4b), that is, the amount of leaf area in relation to the xylem's secondary growth in the last season, significantly decreased with ΔL .

Axial scaling of A_L vs A_X along the branch

For the branches in two regions (NL and FI_S), we analyzed the effect of axial length on the $\log_{10} A_L$ vs $\log_{10} A_X$ relationship. Pairwise association of $\log_{10} A_L$ vs $\log_{10} A_X$ data from sampling points along the longitudinal branch axis revealed that the fitting line was much steeper than that assessed for the 70-cm data only, that is, $b=0.94$ vs $b=0.58$ (Table 2; cf. Fig. 2b with Fig. 2a).

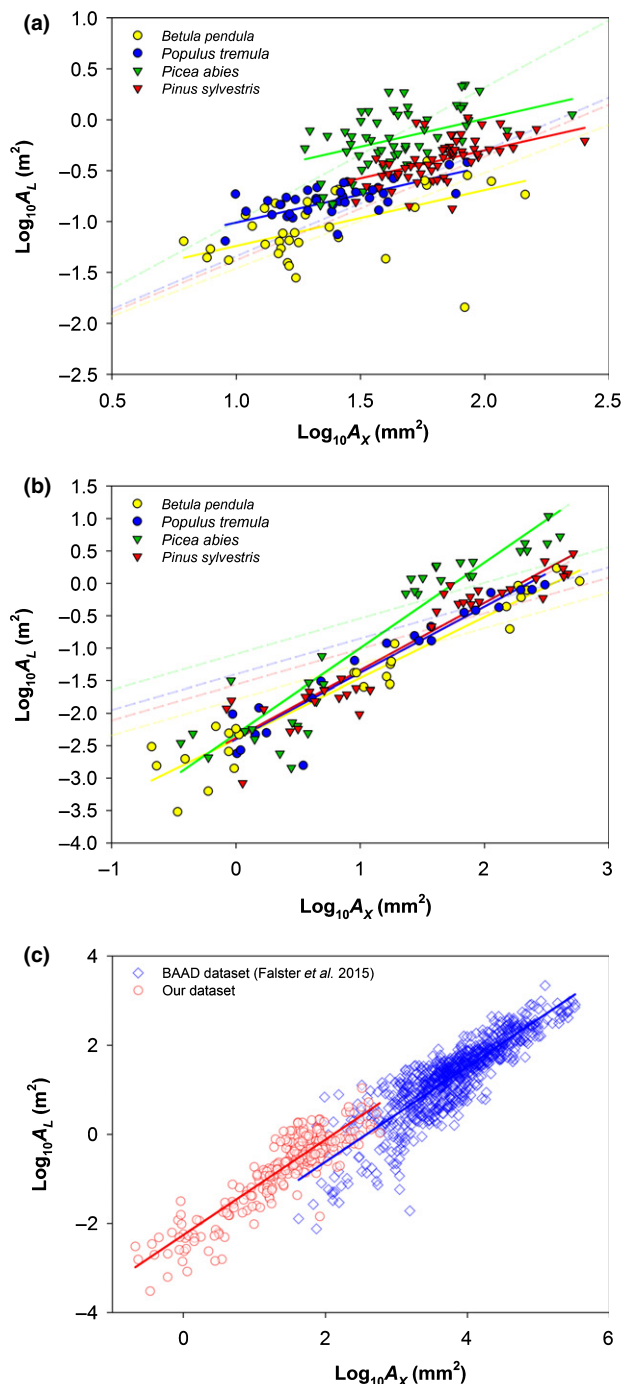


Fig. 2 Relationship of \log_{10} -transformed leaf area ($\log_{10} A_L$) vs \log_{10} -transformed xylem area ($\log_{10} A_X$). (a) Relationship assessed for the data measured at the distance of $L=70$ cm from the apex ('single point' scaling). Solid lines represent the linear fittings according to the model output (Table 2a); dashed lines in background (shaded) represent the fittings reported for Fig. 2(b). (b) Relationship assessed for the data measured at different distances from the apex ('axial' scaling). Solid lines represent the linear fittings according to the model output (Table 2b); dashed lines in background (shaded) are the fittings reported for Fig. 2(a). (c) Relationship assessed for all our branch data ('single points' and 'axial' measurements) and the \log_{10} -transformed data of total A_L of trees and their functional xylem (i.e. sapwood) area at the stem base from BAAD (Falster *et al.*, 2015). Solid lines represent the linear fittings according to the model output (Table 2c).

Table 2 Statistics of selected models for allometric relationships between leaf area (A_L) and xylem area (A_X) at three different scales

| Model information | Covariates and fixed effects | Estimate and differences (\pm SE) | t -value | P | |
|-------------------------|------------------------------|--|--------------------------------|--------------------------------|----------|
| (a) | 70 cm branch | | | | |
| | $R^2 = 0.75$ | Intercept (y_0) | $-1.74 (\pm 0.119)$ | -14.7 | <0.001 |
| | $df = 176$ | $\log_{10} A_X$ (β : slope) | $0.58 (\pm 0.077)$ | 7.6 | <0.001 |
| | Species | <i>B. pendula</i> ² | y_0^a | - | - |
| | | <i>P. tremula</i> | $y_0 + 0.21 (\pm 0.053)^b$ | 3.9 | <0.001 |
| | | <i>P. sylvestris</i> | $y_0 + 0.36 (\pm 0.062)^c$ | 5.8 | <0.001 |
| | | <i>P. abies</i> | $y_0 + 0.67 (\pm 0.057)^d$ | 11.7 | <0.001 |
| | | Region ^{1,5} | FI_N | $y_0 - 0.10 (\pm 0.065)^{a,b}$ | -1.59 |
| | | FI_S | $y_0 - 0.01 (\pm 0.062)^{a,b}$ | -0.07 | |
| | | NL | $y_0 + 0.02 (\pm 0.061)^b$ | 0.34 | |
| | | CZ | $y_0 - 0.13 (\pm 0.061)^a$ | -2.2 | |
| | | CH ³ | $y_0^{a,b}$ | - | |
| | IT | $y_0 - 0.11 (\pm 0.067)^{a,b}$ | -1.63 | | |
| | POR | $y_0 - 0.22 (\pm 0.087)^a$ | -2.52 | | |
| (b) | 2–200 cm branch | | | | |
| | $R^2 = 0.89$ | Intercept (y_0) | $-2.4 (\pm 0.088)$ | -27.7 | <0.001 |
| | $df = 158$ | $\log_{10} A_X$ (β : slope) | $0.94 (\pm 0.062)$ | 15.2 | <0.001 |
| | Species | <i>B. pendula</i> ² | y_0^a | - | - |
| | | <i>P. tremula</i> | $y_0 + 0.00 (\pm 0.154)^a$ | 0.0 | n.s. |
| | | <i>P. sylvestris</i> | $y_0 + 0.02 (\pm 0.143)^a$ | 0.1 | n.s. |
| | | <i>P. abies</i> | $y_0 + 0.08 (\pm 0.129)^a$ | 0.6 | n.s. |
| | Interactions | A_X : <i>B. pendula</i> ² | β^a | | |
| | | A_X : <i>P. tremula</i> | $\beta + 0.08 (\pm 0.108)^a$ | | n.s. |
| | | A_X : <i>P. sylvestris</i> | $\beta + 0.10 (\pm 0.093)^a$ | | n.s. |
| A_X : <i>P. abies</i> | | $\beta + 0.38 (\pm 0.090)^b$ | | <0.001 | |
| (c) | Branches and trees | | | | |
| | $R^2 = 0.87$ | Intercept (y_0) | $-2.26 (\pm 0.040)$ | -56.5 | <0.001 |
| | $df = 1011$ | $\log_{10} A_X$ (β : slope) | $1.07 (\pm 0.020)$ | 54.4 | <0.001 |
| Entity | Tree ⁴ | $y_0 - 0.50 (\pm 0.053)$ | -9.3 | <0.001 | |

For model selection, see Supporting Information Table S1. (a) The selected model equals $\log_{10} A_L = \log_{10} A_X + \text{Species} + \text{Region}$ for the analysis of branches sampled at $L = 70$ cm of four tree species in different regions across Europe (Fig. 2a). (b) The selected model equals $\log_{10} A_L = \log_{10} A_X \times \text{Species}$ for the axial patterns in branches, based on observation from 2 to 200 cm from the apex in 2 sites, NL and FI_S (see Fig. 2b). (c) The selected model equals $\log_{10} A_L = \log_{10} A_X + \text{entity}$ for the branch datasets of (a) and (b) combined with the BAAD data (Falster *et al.*, 2015) for the total leaf area (A_L) and functional xylem (i.e. sapwood) area ($A_X = A_S$) in entire trees. CH, Switzerland; CZ, Czech Republic; FI_N, _S, Finland North and South; IT, Italy; NL, the Netherlands; POR, Portugal.

¹Region – as an additional categorical variable (not in interaction with species), improved the model marginally ($R^2 = 0.73$ to $R^2 = 0.75$), but significantly (see Table S1).

²*Betula pendula* was taken as the reference species and equals the effect of intercept (y_0) and/or slope (β : $\log_{10} A_X$ effect).

³CH was taken as a reference country, and equals the intercept (y_0).

⁴Branch was taken as the reference entity and equals the intercept (y_0). Significant differences between tree species or regions (see Fig. 3) are indicated by different letters.

⁵Differences between species or regions were based on a Tukey honest significant difference *post-hoc* test, and those with region were similar to a test on the residuals of the model excluding region effects (see Table S1).

Our test for possible species and regional effects showed that the slope of the relationship was affected only by species, whereas the y -intercept was unaffected by species and region (Table 2). The slope was steeper for *P. abies* (1.32) than for the other species, but did not significantly differ across *P. sylvestris* (1.04), *P. tremula* (1.02) or *B. Pendula* (0.94) (Tables 2, S1).

Axial scaling: branches vs trees

We analyzed the differences in the scaling of $\log_{10} A_L$ vs $\log_{10} A_X$ between our branches and the entire trees in the BAAD database (Falster *et al.*, 2015), where the functional xylem area was limited to that of sapwood (Table 2; Fig. 2c). Our test revealed that the y -intercept was lower for trees in the BAAD database than in our branches, but they shared a similar slope assessed as $b = 1.1$. This

means that a unit of sapwood area at the stem base can supply a proportionally smaller distal leaf area compared to branches (Fig. 2c).

Discussion

We investigated the variation of leaf area to xylem area for two conifer and two broadleaved tree species over a 27°-wide latitudinal gradient across Europe, which covers the major range distribution of these species from boreal, temperate to Mediterranean regions. We found a convergent scaling of leaf area (A_L) vs xylem area (A_X) in branches sampled at standard distance from the apex ($L = 70$ cm) to an exponent of $b = 0.58$ in all analyzed species. Such a value very much differs from the isometric scaling ($b \sim 1$) found for branches sampled from 2 to 200 cm along the

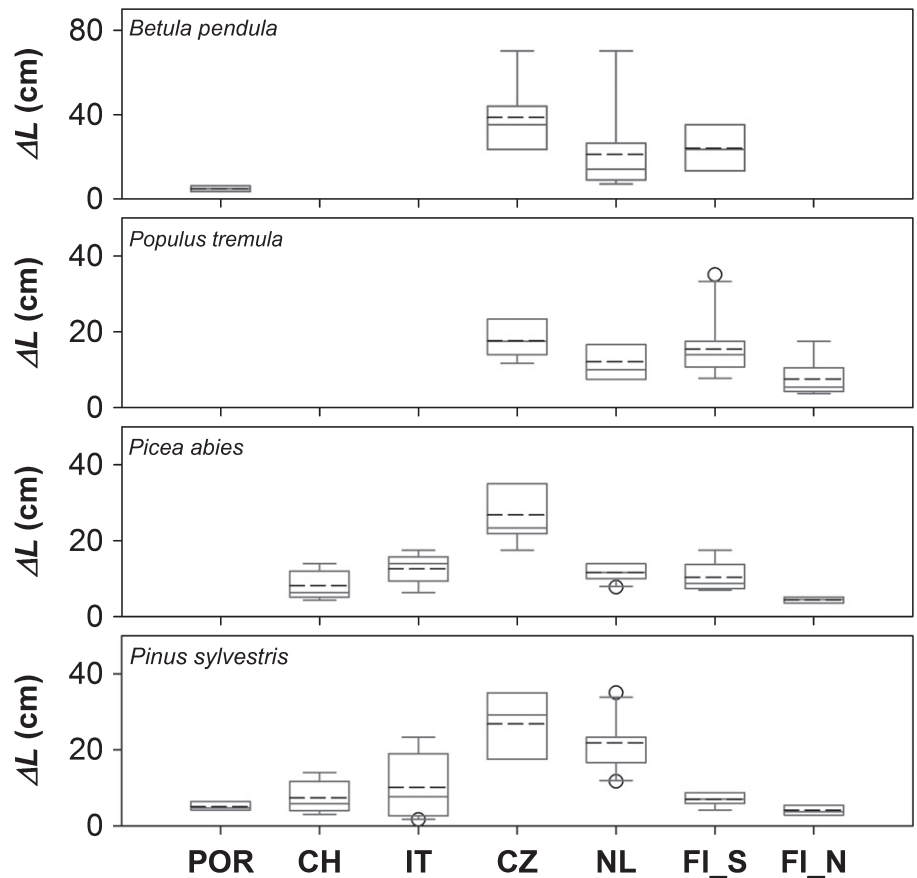


Fig. 3 Boxplot of the variation of the branch elongation rate (ΔL) at the different regions across the latitudinal transect for the different species. Boxes provide the median and 25% and 75% quantiles, and the bars add the range for 10% and 90% quantiles. Dashed lines in boxes represent the mean, and circles are individual observations outside the 10–90 quantile range.

longitudinal branch axis and for trees of different size from the global BAAD database (Falster *et al.*, 2015). Species differed in the y -intercept of the scaling ($y_0 = \log_{10} a$ in Eqn 1), and region effects were only minor and could not be explained by climatic variables. We further discuss how differential allocation between leaves and xylem acts as a mechanism underlying the observed similar balances across trees, despite their differences in growth rate and environmental conditions.

We hypothesized that trees of different species are selected with restricted combinations of A_L and A_S (i.e. structural balances) in branches, thus expecting the convergence towards a similar exponent (b) for the scaling relationship between A_L and A_S . We tested this hypothesis using the observed scaling relationships assessed for the branches sampled at the fixed distance of $L = 70$ cm from the apex. The species differed in the allometric constant (y -intercept), but indeed converged to the same scaling exponent ($b = 0.58$) irrespective of region or species (Figs 2a, S1; Table 2). Differences in allometric constant indicated that conifers have a larger A_L associated with a given A_X than angiosperms, reflecting either their lower physiological potential (including, e.g., stomatal conductance and photosynthetic capacity; Brodribb *et al.*, 2005) or the longer lifespan of needles than angiosperm leaves. The scaling exponent of all species of $b = 0.58$ is remarkably lower than isometry ($b = 1$), meaning that our branches differed mainly in A_X and less so in A_L . Instead, isometry was expected and shown for branches of the same species sampled from 2 cm to 2 m from the apex ($b = 0.94$) and for trees of

different size and different species ($b = 1.07$) from the global BAAD database (Falster *et al.*, 2015). Overall, the structural balance (i.e. the $A_L : A_X$ ratio) of our 70-cm-branches was rather variable (Fig. 4a). Differently from what is reported in other studies (e.g. Mencuccini & Grace, 1995; Martínez-Vilalta *et al.*, 2009; Sellin *et al.*, 2017; Guérin *et al.*, 2018), the differences in $A_L : A_X$ ratio could not be explained by local growing conditions (Table 2; Figs 4a, S1). Instead, the scaling of A_L vs A_X converged towards a similar exponent ($b = 0.58$), independent of regional average climatic conditions (Table 2; Figs 4a, S1), thus suggesting that selection favored restricted combinations of A_L and A_X in branches. Notably, this slope of $b < 1$ would suggest that the absolute amount of A_L vs A_X can change, even though their ‘functional’ covariation along the longitudinal branch axis is maintained ($b \sim 1$) (Fig. 2b; further discussed below).

We observed that the 70 cm branches varied in growth, with branches with slower extension growth (ΔL) mainly in our Southern and Northern latitudinal extremes (Fig. 3). Those branches with slow ΔL had greater leaf area relative to outer xylem ring area than branches with higher ΔL , suggesting that slower growing branches annually allocated more carbon resources into leaf than to xylem area (Fig. 4b). This result is in agreement with the recent hypothesis that a slow branch elongation rate allows for the maintenance of a constant leaf-specific conductance (here simplified as the leaf area to xylem area ratio, Fig. 4a) at low carbon costs, as a greater number of inner sapwood rings produced over multiple years contribute to the

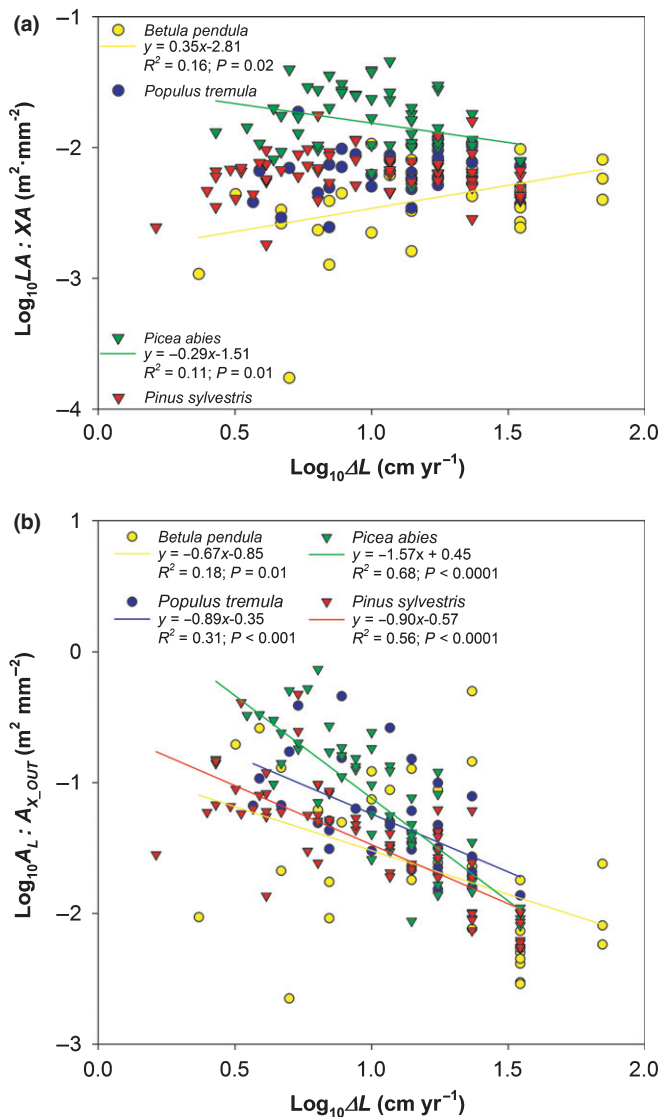


Fig. 4 Effects of branch elongation rate (ΔL) on branch (a) structure and (b) allocation. (a) Relationship between the \log_{10} -transformed ratio of $A_L : A_X$ and $\log_{10} \Delta L$. (b) Relationship between the \log_{10} -transformed ratio of A_L and the area of the outmost xylem ring (A_{X_OUT}). Solid lines represent the ordinary least squares regression lines fitting the data.

functional sapwood of the whole branch (Petit *et al.*, 2016; Sterck & Zweifel, 2016).

In line with our expectation, the A_L vs A_X scaling for branches sampled from 2 to 200 cm from the apex was nearly isometric ($b \sim 1$) apart from for *P. abies* ($b > 1$). This was possibly because this species accumulates its long-lived needles over greater distances from the apex to the base of the branch. Moreover, the close to isometric scaling was similar to that of trees in the BAAD dataset (Falster *et al.*, 2015; Fig. 2c). This implies that the covariation of A_L and A_X along the longitudinal axis is similar for both branches and stems. Our results are in agreement with the commonly reported isometry between A_L and sapwood area assessed for trees or branches of different sizes (Grier & Waring, 1974; Kaufmann & Troendle, 1981; Shelburne *et al.*, 1993). This implies that selection favored individuals with A_L and A_X

increasing in equal proportion to one another ($b \sim 1$) along the longitudinal axis of both branches and stems, likely to guarantee an efficient water transport through the xylem to sustain leaf transpiration (Enquist *et al.*, 1998).

However, we found an offset in the y -intercept, according to which trees have a higher sapwood area per unit of distal leaf area at the stem base compared to distal branches (Sellin & Kopper, 2006). The area of conducting xylem (i.e. sapwood) commonly increases from the top of the stem downwards to the base (van der Sande *et al.*, 2013) because of the progressive increase in the xylem pathways belonging to lateral branches (Bettiati *et al.*, 2012) and in lumen area of xylem conduits (Anfodillo *et al.*, 2013; Olson *et al.*, 2014), but also because a relatively wider sapwood towards the stem base confers stronger resistance against buckling (Niklas, 1995; Larjavaara & Muller-Landau, 2010), or higher conductive and storage capacity (McDowell *et al.*, 2002). Nonetheless, the metabolically active sapwood area at the stem base could be easily overestimated for technical reasons (Bieker & Rust, 2010).

Our scaling relationship observed for 70-cm-long branches provides novel evidence that trees of different species adapt their structural balance between leaf and xylem area in a similar way (with $b = 0.58$). Remarkably, we found only minor regional effects on this relationship, and those effects were not consistently explained by climatic factors. Branches nevertheless differed considerably in extension growth across regions, and it appeared that differential annual allocation between leaves and xylem was underlying their similar scaling in leaf area and xylem area. These results show that the slow branch elongation allowing for the maintenance of a constant leaf-specific conductance at low carbon costs, as shown for two local populations (Petit *et al.*, 2016; Sterck & Zweifel, 2016), also appears for different tree species on a continental scale. We call for further investigation of such convergence in structural balances (A_L vs A_X) across regions and species, which may pose simple principles of structure, growth and allocation that could be integrated in models aiming at predicting plant and vegetation responses to the ongoing changing climate.






Acknowledgements

This article is based upon work from COST Action FP1106 STReESS, supported by COST (European Cooperation in Science and Technology). G.P. was funded by the University of Padova (60A08-2852/15), G.v.A. by the Swiss State Secretariat for Education, Research and Innovation SERI (SBFI C14.0104), A.L. and T.H. by the Academy of Finland (268342, 272041), T.J. by the Japan Society for the Promotion of Science (JSPS KAKENHI no. 26-04395), M.P. by EU Life Programme (LIFE12 ENV/FI/000409), R.L.-d.-V. by Portuguese Fundação para a Ciência e a Tecnologia (FCT; SFRH/BPD/86938/2012), R.L.P. by the Swiss National Science Foundation project, LOTFOR (no. 150205), E.M.R.R. by the EU (Marie Curie IF fellowship, no. 659191) and the Research Foundation – Flanders (FWO, Belgium). We warmly thank Jordi Martínez-Vilalta and Maurizio Mencuccini for their wise comments and suggestions.

Author contributions

F.S. coordinated the experimental design of plots across Europe; G.P., G.v.A., A.L.P., M.C.C., P.C., R.G., L.G., T.H., T.J., A.L., R.L-d-V., M.P., R.L.P., M.S., J.U. and F.S. collected samples in the field; G.P., G.v.A., N.K., S.L., A.L.P., A.C., J.G., M.L., E.M.R.R., S.R.J., M.S. and J.V.C. conducted the anatomical measurements; R.L.P. conducted the needle area measurements for the conifers; G.P., G.v.A., N.K., A.L.P. and F.S. performed the statistical analyses; G.P. wrote the manuscript in collaboration with F.S.; G.P., G.v.A., N.K., S.L., A.L.P., T.A., M.C.C., H.C., P.C., A.C., S.D., R.G., J.G., L.G., T.H., T.J., M.L., A.L., R.L-d-V., M.P., R.L.P., E.M.R.R., S.R.J., M.S., K.S., J.U., J.V.C. and F.S. contributed by discussing and reviewing the drafts and final version.

ORCID

Giai Petit  <http://orcid.org/0000-0002-6546-7141>
 Silvia Lechthaler  <http://orcid.org/0000-0002-3670-1154>
 Angela Luisa Prendin  <http://orcid.org/0000-0002-5809-7314>
 Paul Copini  <http://orcid.org/0000-0002-5547-2609>
 Sylvain Delzon  <http://orcid.org/0000-0003-3442-1711>

References

- Anderson G, Bancroft J. 2002. Tissue processing and microtomy including frozen. In: Bancroft J, Gamble JD, eds. *Theory and practice of histological techniques*. London, UK: Churchill Livingstone, 87–107.
- Anfodillo T, Petit G, Crivellaro A. 2013. Axial conduit widening in woody species: a still neglected anatomical pattern. *IAWA Journal* 34: 352–364.
- Anfodillo T, Petit G, Sterck F, Lechthaler S, Olson ME. 2016. Allometric trajectories and “stress”: a quantitative approach. *Frontiers in Plant Science* 7: 1681.
- von Arx G, Carrer M. 2014. ROXAS – a new tool to build centuries-long tracheid-lumen chronologies in conifers. *Dendrochronologia* 32: 290–293.
- von Arx G, Crivellaro A, Prendin AL, Čufar K, Carrer M. 2016. Quantitative wood anatomy – practical guidelines. *Frontiers in Plant Science* 7: 781.
- Banavar JR, Maritan A, Rinaldo A. 1999. Size and form in efficient transportation networks. *Nature* 399: 130–132.
- Bettiati D, Petit G, Anfodillo T. 2012. Testing the equi-resistance principle of the xylem transport system in a small ash tree: empirical support from anatomical analyses. *Tree Physiology* 32: 171–177.
- Bieker D, Rust S. 2010. Non-destructive estimation of sapwood and heartwood width in Scots pine (*Pinus sylvestris* L.). *Silva Fennica* 44: 267–273.
- Brodribb TJ, Holbrook NM, Zwieniecki MA, Palma B. 2005. Leaf hydraulic capacity in ferns, conifers and angiosperms: impacts on photosynthetic maxima. *New Phytologist* 165: 839–846.
- Buckley TN, Roberts DW. 2006. How should leaf area, sapwood area and stomatal conductance vary with tree height to maximize growth? *Tree Physiology* 26: 145–157.
- Carrer M, von Arx G, Castagneri D, Petit G. 2015. Distilling allometric and environmental information from time series of conduit size: the standardization issue and its relationship to tree hydraulic architecture. *Tree Physiology* 35: 27–33.
- Cochard H. 2006. Cavitation in trees. *Comptes Rendus Physique* 7: 1018–1026.
- Enquist BJ, Brown JH, West GB. 1998. Allometric scaling of plant energetics and population density. *Nature* 395: 163–165.
- Falster DS, Duursma RA, Ishihara MI, Barneche DR, FitzJohn RG, Vårhammar A, Aiba M, Ando M, Anten N, Aspinwall MJ *et al.* 2015. BAAD: a Biomass And Allometry Database for woody plants. *Ecology* 96: 1445.
- Gleason SM, Westoby M, Jansen S, Choat B, Hacke UG, Pratt RB, Bhaskar R, Brodribb TJ, Bucci SJ, Cao K-F *et al.* 2016. Weak tradeoff between xylem safety and xylem-specific hydraulic efficiency across the world’s woody plant species. *New Phytologist* 209: 123–136.
- Grier CC, Waring RH. 1974. Notes: conifer foliage mass related to sapwood area. *Forest Science* 20: 205–206.
- Guérin M, Martin-Benito D, von Arx G, Andreu-Hayles L, Griffin KL, Hamdan R, McDowell NG, Muscarella R, Pockman W, Gentine P. 2018. Interannual variations in needle and sapwood traits of *Pinus edulis* branches under an experimental drought. *Ecology and Evolution* 8: 1655–1672.
- Hacke UG, Sperry JS. 2001. Functional and ecological xylem anatomy. *Perspectives in Plant Ecology Evolution and Systematics* 4: 97–115.
- Hacke UG, Sperry JS, Wheeler JK, Castro L. 2006. Scaling of angiosperm xylem structure with safety and efficiency. *Tree Physiology* 26: 689–701.
- Hacke UG, Spicer R, Schreiber SG, Plavcová L. 2017. An ecophysiological and developmental perspective on variation in vessel diameter. *Plant, Cell & Environment* 40: 831–845.
- Kaufmann MR, Troendle CA. 1981. The relationship of leaf area and foliage biomass to sapwood conducting area in four subalpine forest tree species. *Forest Science* 27: 477–482.
- Larjavaara M, Muller-Landau HC. 2010. Rethinking the value of high wood density. *Functional Ecology* 24: 701–705.
- Martínez-Vilalta J, Cochard H, Mencuccini M, Sterck F, Herrero A, Korhonen JFJ, Llorens P, Nikinmaa E, Nolè A, Poyatos R *et al.* 2009. Hydraulic adjustment of Scots pine across Europe. *New Phytologist* 184: 353–364.
- McDowell N, Barnard H, Bond BJ, Hinckley T, Hubbard RM, Ishii H, Kostner B, Magnani F, Marshall JD, Meinzer FC *et al.* 2002. The relationship between tree height and leaf area: sapwood area ratio. *Oecologia* 132: 12–20.
- McDowell N, Pockman WT, Allen CD, Breshears DD, Cobb N, Kolb T, Plaut J, Sperry J, West A, Williams DG *et al.* 2008. Mechanisms of plant survival and mortality during drought: why do some plants survive while others succumb to drought? *New Phytologist* 178: 719–739.
- Mencuccini M. 2014. Temporal scales for the coordination of tree carbon and water economies during droughts. *Tree Physiology* 34: 439–442.
- Mencuccini M, Grace J. 1995. Climate influences the leaf area/sapwood area ratio in Scots pine. *Tree Physiology* 15: 1–10.
- Mencuccini M, Höltta T, Petit G, Magnani F. 2007. Sanio’s laws revisited. Size-dependent changes in the xylem architecture of trees. *Ecology Letters* 10: 1084–1093.
- Mitchell PJ, O’Grady AP, Tissue DT, Worledge D, Pinkard EA. 2014. Coordination of growth, gas exchange and hydraulics define the carbon safety margin in tree species with contrasting drought strategies. *Tree Physiology* 34: 443–458.
- Nardini A, Lo Gullo MA, Salleo S. 2011. Refilling embolized xylem conduits: is it a matter of phloem unloading? *Plant Science* 180: 604–611.
- Niklas KJ. 1995. Size-dependent allometry of tree height, diameter and trunk taper. *Annals of Botany* 75: 217–227.
- Olson ME, Anfodillo T, Rosell JA, Petit G, Crivellaro A, Isnard S, León-Gómez C, Alvarado-Cárdenas LO, Castorena M. 2014. Universal hydraulics of the flowering plants: vessel diameter scales with stem length across angiosperm lineages, habits and climates. *Ecology Letters* 17: 988–997.
- Petit G, Anfodillo T. 2009. Plant physiology in theory and practice: an analysis of the WBE model for vascular plants. *Journal of Theoretical Biology* 259: 1–4.
- Petit G, Pfautsch S, Anfodillo T, Adams MA. 2010. The challenge of tree height in *Eucalyptus regnans*: when xylem tapering overcomes hydraulic resistance. *New Phytologist* 187: 1146–1153.
- Petit G, Savi T, Consolini M, Anfodillo T, Nardini A. 2016. Interplay of growth rate and xylem plasticity for optimal coordination of carbon and hydraulic economies in *Fraxinus ornus* trees. *Tree Physiology* 36: 1310–1319.
- Prendin AL, Petit G, Carrer M, Fonti P, Björklund J. 2017. New research perspectives from a novel approach to quantify tracheid wall thickness. *Tree Physiology* 37: 976–983.
- R Development Core Team. 2014. *R: a language and environment for statistical computing*. Vienna, Austria: R Foundation for Statistical Computing. <http://www.R-project.org/>.

- van der Sande MT, Poorter L, Schnitzer SA, Markesteijn L. 2013. Are lianas more drought-tolerant than trees? A test for the role of hydraulic architecture and other stem and leaf traits. *Oecologia* 172: 961–972.
- Sellin A, Alber M, Kupper P. 2017. Increasing air humidity influences hydraulic efficiency but not functional vulnerability of xylem in hybrid aspen. *Journal of Plant Physiology* 219: 28–36.
- Sellin A, Kupper P. 2006. Spatial variation in sapwood area to leaf area ratio and specific leaf area within a crown of silver birch. *Trees* 20: 311–319.
- Shelburne VB, Hedden RL, Allen RM. 1993. The effect of site, stand density, and sapwood permeability on the relationship between leaf area and sapwood area in loblolly pine (*Pinus taeda* L.). *Forest Ecology and Management* 58: 193–209.
- Spicer R, Gartner BL. 2001. The effects of cambial age and position within the stem on specific conductivity in Douglas-fir (*Pseudotsuga menziesii*) sapwood. *Trees* 15: 222–229.
- Sterck F, Zweifel R. 2016. Trees maintain a similar conductance per leaf area through integrated responses in growth, allocation, architecture and anatomy. *Tree Physiology* 36: 1307–1309.
- Tullus A, Kupper P, Sellin A, Parts L, Söber J, Tullus T, Löhmus K, Söber A, Tullus H. 2012. Climate change at Northern latitudes: rising atmospheric humidity decreases transpiration, N-uptake and growth rate of hybrid aspen. *PLoS ONE* 7: e42648.
- Tyree MT, Zimmermann MH. 2002. *Xylem structure and the ascent of sap*. Berlin, Germany: Springer.
- West GB, Brown JH, Enquist BJ. 1999. A general model for the structure and allometry of plant vascular systems. *Nature* 400: 664–667.
- Zuur A, Ieno EN, Walker N, Saveliev AA, Smith GM. 2009. *Mixed effects models and extensions in ecology with R*. New York, NY, USA: Springer.
- Zweifel R, Zimmermann L, Newbery DM. 2005. Modeling tree water deficit from microclimate: an approach to quantifying drought stress. *Tree Physiology* 25: 147–156.

Supporting Information

Additional Supporting Information may be found online in the Supporting Information tab for this article:

Fig. S1 Effects of regional climate and branch elongation rate (ΔL) on the residuals of the assessed relationship $\log_{10} A_L$ vs $\log_{10} A_X$ for the branches sampled at 70 cm from the apex.

Table S1 Best model selection for the relationships $\log_{10} A_L$ vs $\log_{10} A_X$, accounting for the possible effects of species, region and entity (branch/tree)

Please note: Wiley Blackwell are not responsible for the content or functionality of any Supporting Information supplied by the authors. Any queries (other than missing material) should be directed to the *New Phytologist* Central Office.



About New Phytologist

- *New Phytologist* is an electronic (online-only) journal owned by the New Phytologist Trust, a **not-for-profit organization** dedicated to the promotion of plant science, facilitating projects from symposia to free access for our Tansley reviews and Tansley insights.
- Regular papers, Letters, Research reviews, Rapid reports and both Modelling/Theory and Methods papers are encouraged. We are committed to rapid processing, from online submission through to publication 'as ready' via *Early View* – our average time to decision is <26 days. There are **no page or colour charges** and a PDF version will be provided for each article.
- The journal is available online at Wiley Online Library. Visit www.newphytologist.com to search the articles and register for table of contents email alerts.
- If you have any questions, do get in touch with Central Office (np-centraloffice@lancaster.ac.uk) or, if it is more convenient, our USA Office (np-usaoffice@lancaster.ac.uk)
- For submission instructions, subscription and all the latest information visit www.newphytologist.com